Biosensors and Bioelectronics 114 (2018) 72–77

Contents lists available at ScienceDirect

Biosensors and Bioelectronics

journal homepage: www.elsevier.com/locate/bios

Analogous modified DNA probe and immune competition method-based electrochemical biosensor for RNA modification

Tao Dai[a], Qinli Pu[a], Yongcan Guo[b], Chen Zuo[a], Shulian Bai[a], Yujun Yang[a], Dan Yin[a], Yi Li[a], Shangchun Sheng[c], Yiyi Tao[a], Jie Fang[a], Wen Yu[a], Guoming Xie[a,*]

[a] Key Laboratory of Laboratory Medical Diagnostics, Ministry of Education, Department of Laboratory Medicine, Chongqing Medical University, No. 1 Yi Xue Yuan Road, Chongqing 400016, PR China
[b] Clinical Laboratory of Traditional Chinese Medicine Hospital Affiliated to Southwest Medical University, Luzhou 646000, PR China
[c] Clinical Laboratory of the Affiliated Hospital of Chengdu University, Chengdu 610000, PR China

ARTICLE INFO

Keywords:
Electrochemical immunosensor
RNA modifications
N6-methyladenosine
Analogous modified DNA probe

ABSTRACT

N6-methyladenosine (m6A), one of the most abundant RNA methylation which is ubiquitous in eukaryotic RNA, plays vital roles in many biological progresses. Therefore, the rapid and accurate quantitative detection of m6A is particularly important for its functional research. Herein, a label-free and highly selective electrochemical immunosensor was developed for the detection of m6A. The method is established on that the anti-m6A-Ab can recognize both m6A-RNA and m6A-DNA. An analogous modified DNA probe (L1) serves as a signal molecule, by competing with m6A-RNA for binding to Abs to broaden the linear range. The detection of m6A-RNA by this method is unaffected by the lengths and base sequences of RNA. Under optimal conditions, the proposed immunosensor presented a wide linear range from 0.05 to 200 nM with a detection limit as low as 0.016 nM (S/N = 3). The specificity and reproducibility of the method are satisfactory. Furthermore, the developed immunosensor was validated for m6A determination in human cell lines. Thus, the immunosensor provides a promising platform for m6A-RNA detection with simplicity, high specificity and sensitivity.

1. Introduction

Epigenetics is a genetics branch discipline that studies heritable changes in gene expression without gene nucleotide sequence change. In the central dogma, RNA is a bond between DNA and protein, not only for the transmission of genetic information, but also for a variety of post-transcriptional regulatory functions. Over the past decades, researchers have found more than 150 types of chemical modifications on RNA (Helm and Motorin, 2017). These modifications have greatly expanded the diversity of RNA functions and genetic information, and have a very important regulatory role in gene expression (Gilbert et al., 2016), disease occurrence (Bellodi et al., 2013), growth and development (Kan et al., 2017), immune regulation (Slotkin and Nishikura, 2013) and so on. Therefore, the detection of RNA modifications not only has very important significance to epigenetics research, but also has great potential clinical application values with respect to disease risk assessment, diagnosis, treatment and precision medical treatment (Chen et al., 2017; Nainar et al., 2016; Vu et al., 2017; Zhang et al., 2016).

N6-methyladenosine (m6A) is one of the most abundant RNA modifications, which is ubiquitous in eukaryotic RNA (Zhang et al., 2017). As is well known that DNA and proteins undergo dynamic and reversible chemical modifications that influence their functions (Meyer and Jaffrey, 2014), the modification of RNA is also dynamically regulated by many methyltransferase such as methyltransferase-like 14 (METTL14) and demethylase like fat mass and obesity-associated proteins (FTO) (Ma et al., 2017; Visvanathan et al., 2018). Accumulative evidences indicate that variant m6A levels exert diverse biological functions in mammals, such as transcription splicing (Zhao et al., 2014), nuclear RNA export (Wang et al., 2014), protein translation control (Wang et al., 2015), and cell fate determination (Geula et al., 2015). The regulatory machinery of m6A modification might be associated with human diseases or cancers (Chandola et al., 2015). In order to understand the relationship between the expression level of m6A in the gene transcripts and its basic functions, it is particularly important to rapidly and accurately detect the m6A. However, the amount of m6A in isolated RNA was estimated to be only 0.1–0.6% in Homo sapiens (Li et al., 2016b), which means only about 3–5 m6A sites in per mRNA not to mention in the total RNA (Klungland and Dahl, 2014). Low abundance of m6A in RNA (m6A-RNA) makes the precise detection difficult.

* Corresponding author.
E-mail addresses: guomingxie@cqmu.edu.cn, xiegm059@foxmail.com (G. Xie).

https://doi.org/10.1016/j.bios.2018.05.018
Received 12 February 2018; Received in revised form 8 May 2018; Accepted 9 May 2018

Moreover, the methylation of adenosine does not change its ability to base pair with thymidine and uracil. Therefore, m6A cannot be detected with standard hybridization or sequencing-based methods. The m6A was first found in 1974, while the research on the biological functions of m6A is greatly lagged due to the lack of reliable and sensitive detection technique.

Some strategies for RNA m6A (m6A-RNA) detection were reported, including thin layer chromatography (TLC) (Jia et al., 2011), liquid chromatography–tandem mass spectrometry (LC–MS/MS) (Yan et al., 2013), high performance liquid chromatography (HPLC) (Narayan et al., 1994), m6A individual-nucleotide-resolution cross-linking and immunoprecipitation (miCLIP) (Linder et al., 2015), chromatin immunoprecipitation followed by sequencing (ChIP-Seq) (Dominissini et al., 2012) and methylated RNA immunoprecipitation followed by sequencing (MeRIP-Seq) (Meyer et al., 2012). However, some of those techniques require labeling RNA with P^{32}, which is harmful to the operator's health and the environment. The other techniques need either expensive or large instruments, or complicated operation steps, or long detection time or skilled personnel, thus greatly limit their applications for rapid detection of m6A.

Electrochemical biosensors have attracted extensive attention and rapid development, due to merits of simple operation, time-saving, low-cost, miniaturized instrument, high sensitivity and selectivity. Up to now, electrochemical technique can be used in many fields, such as environmental pollution (Wang et al., 2017; Zeng et al., 2017), food safety (Lv et al., 2018; Silva et al., 2018), protein (Ji et al., 2017; Zhao et al., 2018), cell (Shen et al., 2016; Tang et al., 2018), and nucleic acid (Li et al., 2016a; Tao et al., 2017; Benvidi and Jahanbani, 2016). Especially, electrochemical technique has been applied to analyze modifications of nucleic acid, including DNA methylation (Gao et al., 2018; Jing et al., 2014). Therefore, the electrochemical method could be a potential technique for m6A-RNA detection, and several works have been done. Yin et al. has developed two electrochemical immunosensors for quantitative detection of m6A with high sensitivity (Yin et al., 2017, 2015), and Benvidi et al. has developed electrochemical impedance methods for DNA detection (Benvidi et al., 2014, 2016). It is a great encouragement for us to develop a simple and label-free electrochemical impedance method to determine m6A-RNA with high specificity.

In this work, we fabricated a simple, label-free, sensitive and selective electrochemical immunosensor for quantitative detection of m6A-RNA shown in Scheme 1. This method based on the specific interaction between antibody (Ab) and antigen (Ag), and the fact that anti-m6A-antibody (anti-m6A-Ab) can recognize both m6A-RNA and DNA m6A (m6A-DNA) (Xiang et al., 2017). First, the histidine-tagged recombinant protein G (his-PG) can firmly bind to the surface of a gold electrode through its histidine tag to form a directional layer, which promotes immobilization of Abs on the surface of the gold electrode. Abs are oriented by the specific interaction of the fragment crystallizable region (Fc) with PG that forces Ab to expose its binding sites to the environment, which can improve the recognization ability and efficiency between Ag and Ab (Casalini et al., 2015). Then m6A-DNA probes (L1), competing with the m6A-RNA in the sample for binding to the Abs, help to broaden the detection range (Nelson et al., 2003). After that, ribonuclease A (RNase A) is used to hydrolyze RNA bound to Abs. Finally the electrochemical impedance spectroscopy (EIS) signal of the electrode is detected and the intensity of the signal is inversely proportional to the amount of m6A- RNA in the sample.

2. Experimental

2.1. Reagents and materials

See Supplementary material.

2.2. Instrumentation

See Supplementary material.

2.3. Preparation of gold electrode

Prior to modification, the gold electrode was polished to mirror-like surface with 0.05 μm Al_2O_3 slurry. Then the gold electrode was sonicated alternatively for 5 min in ultrapure water, and anhydrous ethanol. After that, it was activated in freshly prepared piranha solution (98% H_2SO_4 / 30% H_2O_2, 7:3, v/v) for 5 min and rinsed with ultrapure water thoroughly.

2.4. Immunosensors fabrication

First, 10 μL of 20 μg/mL his-PG was added on the gold electrode and incubated overnight in a 4 °C refrigerator, then rinsed with 10 mM PBS buffer. The obtained electrode was incubated with 10 μL of 20 μg/mL anti-m6A-Ab at 4 °C for 3 h. After rinsed with 10 mM PBS buffer, the electrode was incubated with 10 μL of 0.25% Bovine serum albumin (BSA) at 4 °C for 1 h. Followed rinsing with 10 mM PBS buffer, the anti-m6A-Ab combined with m6A by drop 10 μL of mixed solution which containing different concentrations of targets and 5 nM L1 at room

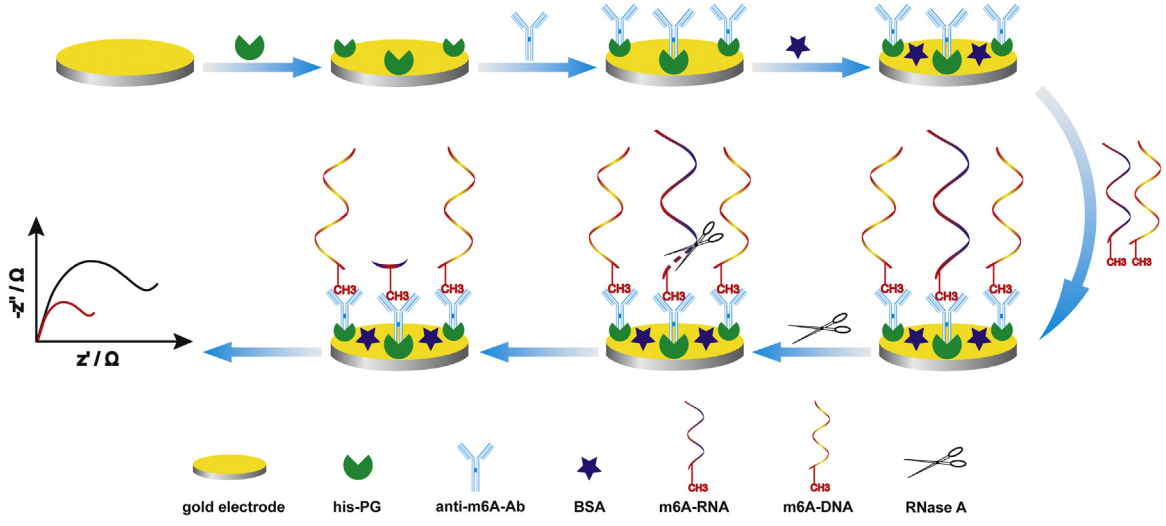

Scheme 1. The procedures of fabricate immunosensor.

temperature (RT, 25 ± 2 °C) for 45 min. Subsequently, the electrode was immersed in 1 μg/mL RNase A at RT for 1 h. Finally, the electrode was thoroughly rinsed with 10 mM PBS buffer.

2.5. Electrochemical detection

The electrochemical signal was detected in the working solution (10 mM PBS, pH 7.4) containing 5 mM $[Fe(CN)_6]^{3-/4-}$ and 0.1 M KCl by EIS with the frequency range of 10^{-1}–10^5 Hz with a signal amplitude of 5 mV.

2.6. Cell culture and total RNA extraction

The human hepatoma cell line HepG-2 and human normal liver cell line L02 were cultured in Dulbecco's Modified Eagle Medium (DMEM) supplemented with 10% (v/v) fetal bovine serum, and penicillin-streptomycin (100 mg/mL) at 37 °C in an incubator containing 5% CO_2. The human bronchial epithelial cell line HBE and human lung cancer cell line A549 were cultured in the same conditions except that, the culture medium was changed to Roswell Park Memorial Institute (RPMI-1640). After 4 days culture, the cells were washed three times with 10 mM PBS buffer. Then the total RNA was extracted by TRIzol reagent according to the manufacturer's recommended protocol, the extraction procedure was shown in Fig. S1. The concentration and purity of the harvested total RNA were tested by NanoDrop 1000 Spectrophotometer and the results were shown in Fig. S2 and Table S2. The values of A260/A280 are very close to 2.0, indicated that the extracted RNA is of high purity (Wang et al., 2010).

3. Results and discussion

3.1. Characterization of the immunosensors

Atomic force microscopy (AFM) is an effective way to distinguish the surface morphological changes of electrode. Fig. 1A showed the topography map of his-PG immobilized on the surface of the gold electrode. Then the anti-m6A-Ab combined to his-PG, there are a lot of hump-like structures, which are consistent with the 'Y' shape of IgG Ab (Fig. 1B). All the Abs have the same orientation, demonstrating that the Abs were oriented immobilized on the electrode by his-PG. After added the m6A-DNA (L1), many ribbons were seen in the top of the hump structures (Fig. 1C), indicating that the m6A-DNAs were captured by anti-m6A-Abs. Therefore, the above results indicated that the Ab can be oriented immobilized on the surface of the gold electrode by his-PG, and the m6A can be captured by the Ab.

Cyclic voltammetry (CV) is an effective method to reveal each step of modification of the working electrode. The cyclic voltammograms shown in Fig. 2A were obtained from the gold electrode in the working solution at a scan rate of 0.1 V/S. Curve a showed a well-defined redox peak, which could be contribute to the good conductivity of the bare gold electrode. The current response decreased after the his-PG immobilized onto the gold electrode (curve b), which was attribute to the his-PG impede the diffusion of $[Fe(CN)_6]^{3-/4-}$ to the surface of electrode and decrease the electron transfer rate. As the electrode was incubated with anti-m6A-Abs the current suffered a decrease (curve c). There is no doubt that this decrease is caused by the modification of Abs on the electrode surface, because of the huge volume of Abs further resistance the diffusion of $[Fe(CN)_6]^{3-/4-}$. After the electrode was incubated with BSA the current suffered a further decrease (curve d), which was mainly caused by the blocking effect of the BSA. Subsequently, the current value decreased successively when m6A-RNA probe P1 (curve e) and m6A-DNA probe L1 (curve f) were captured on the electrode surface, respectively. It could be explained as the electrostatic repulsion between the negatively charged probes and $[Fe(CN)_6]^{3-/4-}$. Then RNase A was used to hydrolyze the P1 on the electrode, compared to the curve e the current has increased, due to the disappearance of electrostatic repulsion (curve g). According to the above results, we confirmed that the fabrication of the proposed immunosensor was successful.

EIS can response to the changes of the electrode surface timely and sensitively. Therefore, it was perfectly used to monitoring the layer-by-layer assembly process. The curve of EIS consists of the semicircle section and linear section, the semicircle section relates to the interface electron transfer resistance (Ret) at high frequencies, and the linear section indicates a diffusion-controlled process in solution at low frequencies. As shown in Fig. 2B, a small semicircle portion showed the excellent electron-transfer capability of the bare gold electrode (curve a). After assembling of his-PG, the Ret value increased from 164 to 1779 Ω (curve b). Due to the resistance, the Ret value increased (curve c) when the anti-m6A-Abs linked with his-PG, indicating that the anti-m6A-Abs were successfully assembled on the gold electrode. After blocked by BSA, the Ret value further increased (curve d). As expected, the Ret value significantly increased after the P1 (curve e) and L1 (curve f) were captured by Abs. With RNase A hydrolysis of P1, the Ret value showed a clear decrease compared to curve e (curve g). Values of the equivalent circuit parameters of the fitting curves for the stepwise fabrication of the biosensor were processed by Zview 2 software. With layer-by-layer assembly, the electrochemical impedance values altered gradually and the changes were consistent with those in the CV method, further proving that the fabrication of the immunosensor is feasible.

3.2. Optimization of experimental parameters

In order to obtain a better performance of the immunosensor, we have optimized several vital parameters, including the immobilization time of Ab, the concentration of L1, the incubation time of L1, and the RNase A hydrolysis time.

Fig. 3A illustrated the effect of Abs incubation time on the electrochemical response of the biosensor. When 10 μL of 20 μg/mL Abs were added on the electrode the electrochemical signals increased as the extension of the immobilization time from 0 to 3 h, and there was a plateau when further extend the immobilization time. Within 3 h, as incubation time increase, more Abs can be immobilized on the electrode surface, leading to higher capture capacity of m6A. As a result, more targets can be captured on the surface of gold electrode thus

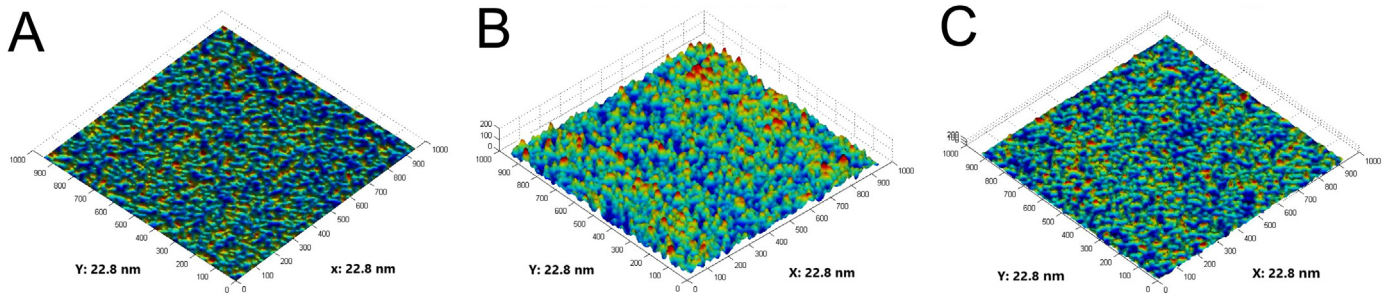

Fig. 1. AFM images of (A) his-PG / Au electrode, (B) anti-m6A-Ab / his-PG / Au electrode and (C) L1 / anti-m6A-Ab / his-PG / Au electrode.

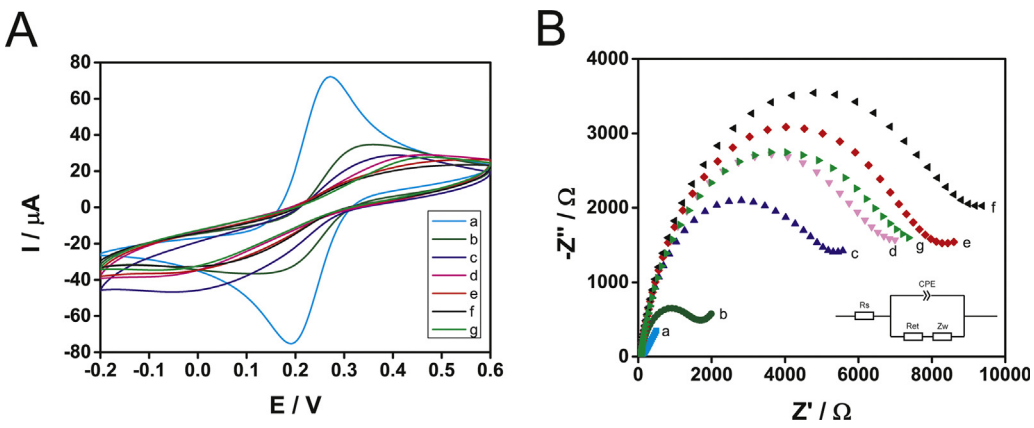

Fig. 2. Electrochemical characterization of the immunosensor. (A) Cyclic voltammetry and (B) Nyquist plots obtained from different electrodes: (a) bare gold electrode, (b) his-PG / Au electrode, (c) anti-m6A-Ab / his-PG / Au electrode, (d) BSA / anti-m6A-Ab / his-PG / Au electrode, (e) P1 / BSA / anti-m6A-Ab / his-PG / Au electrode, (f) L1 / BSA / anti-m6A-Ab / his-PG / Au electrode, (g) RNase A / P1 / BSA / anti-m6A-Ab / his-PG / Au electrode.

increasing the electrochemical response. Nevertheless, when further extending the time, the immobilized Abs tend to saturate, resulting the electrochemical response into a plateau. Therefore, 3 h was selected as the optimum time in this work.

To understand the capture ability of the biosensor to m6A, and to chose a suitable concentration of L1 for subsequent experiment, we investigated the maximum capture concentrations of L1 under the condition of incubation for 1 h at room temperature, as shown in Fig. 3B. The EIS signal gradually increased with the increasing of the concentration of L1 to the limit of 5 nM, but further increasing the concentration had no obvious change. Therefore, in order to ensure that all Abs of the immunosensor can be saturated by m6A in subsequent experiments, 5 nM was chosen as the optimal concentration of L1.

The effect of incubation time of L1 is also a very important condition. As shown in Fig. 3C, the EIS responses at different incubation time (0, 30, 45, 60, and 90 min) were recorded. The signal reached a plateau after incubated 45 min. These results demonstrated that the optimum incubation time of m6A is 45 min.

RNase A hydrolysis of target RNA is a key link for the performance of immunosensor. Fig. 3D showed the variation trend of the EIS signal as the hydrolysis time growing. It is easy to see when the incubation time reaches 60 min or longer, the Ret values had no obvious change. Hence, 60 min was determined as the hydrolysis time.

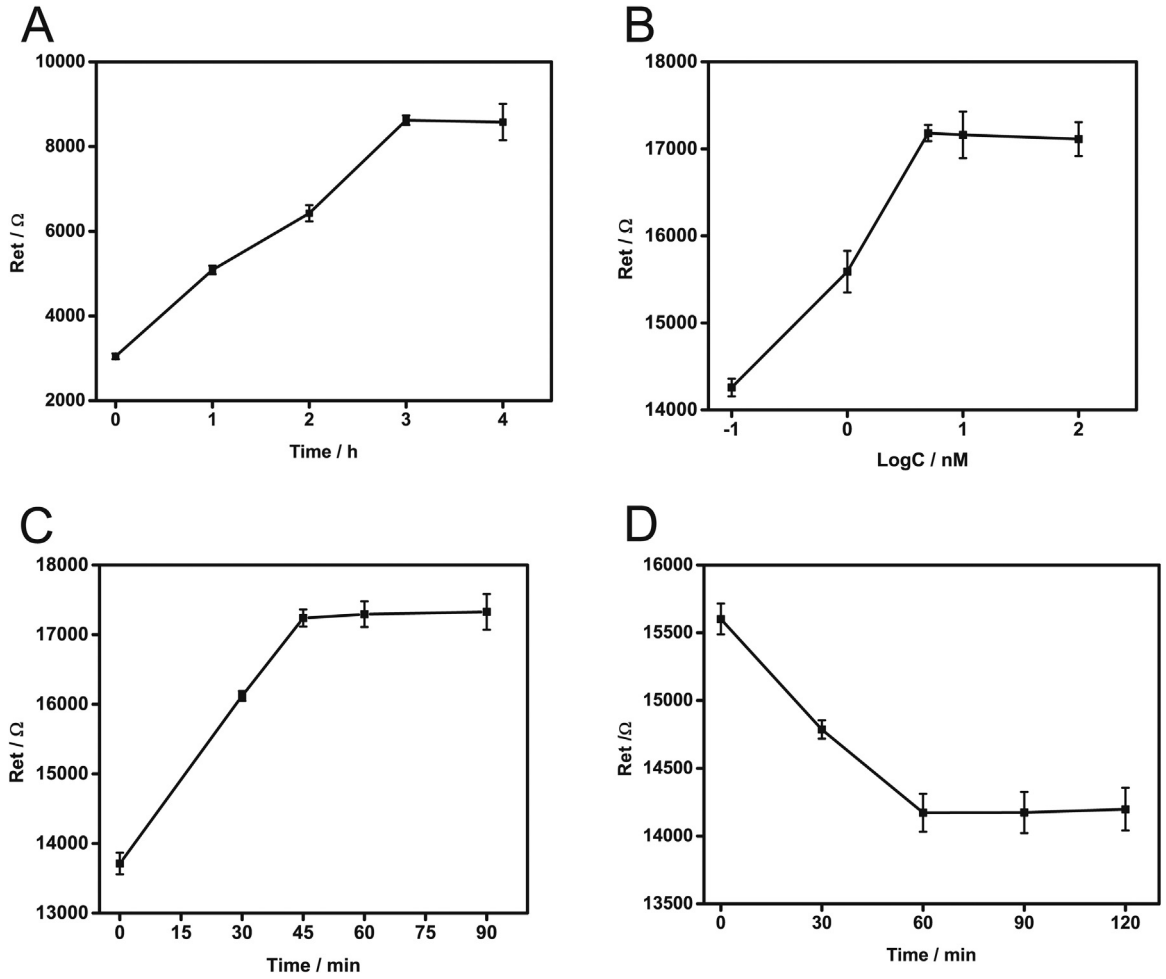

Fig. 3. Experimental condition optimization: (A) Ab immobilization time, (B) L1 concentration, (C) L1 immobilization time, (D) RNase A hydrolysis time.

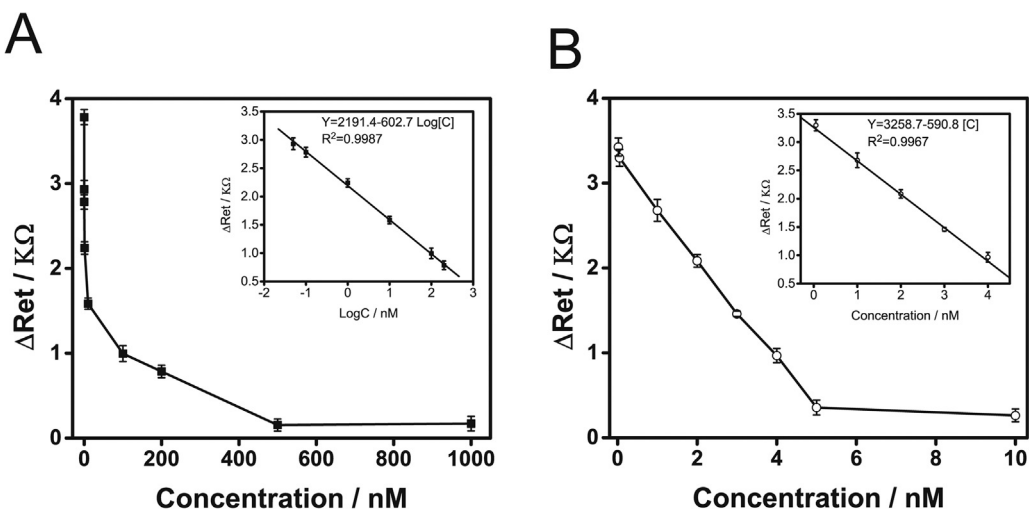

Fig. 4. (A) The Ret values of the electrochemical immuniosensor with M1 at different concentrations of P1: 0.01, 0.05, 0.1, 1, 10, 100, 200, 500, 1000 nM. Inset graph shows the relationship between the Ret value and the logarithm value of P1 concentration (n = 3). (B) The Ret values of the electrochemical immuniosensor with M2 at different concentrations of P1: 0.02, 0.05, 1, 2, 3, 4, 5, 10 nM. Inset graph shows the relationship between the Ret value and the concentration of P1 (n = 3).

3.3. Detection sensitivity and selectivity

In order to obtain an immunosensor with high sensitivity and wide linear range, we compared two different ways of sample addition. The first method is to add m6A-RNA (P1 or target) and 5 nM L1 at the same time (recorded as M1), the second is to sequentially add m6A-RNA and 5 nM L1 (namely M2). Under the optimum experimental conditions, the EIS responses for the different concentrations of P1 are denoted as Ret, the electrical impedance value of the immunosensor (BSA/anti-m6A-Ab/ his-PG/gold electrode) is denoted as R_0. Fig. 4A (M1) and Fig. 4B (M2) reveal the relationship between ΔRet (Ret-R_0) and different concentrations of P1, and the Nyquist diagrams are shown in Fig. S3. In Fig. 4A (M1) the ΔRet values show a good linear relationship with logarithm values of the concentration of P1 in the range from 0.05 to 200 nM. The linear regression equation can be expressed as Y = 2191.4 – 602.7 Log[C], with a correlation coefficient R^2 = 0.9987. The detection limit was calculated to be 0.016 nM (S/N = 3). The calibration curve of M2 also shows a good linear relationship between ΔRet and the concentration of P1 in the range from 0.05 to 4 nM. The linear regression equation can be written as Y = 3258.7 – 590.8 [C], with a correlation coefficient R^2 = 0.9967. The detection limit was calculated to be 0.023 nM (S/N = 3).

Comparing the two methods, we found that M1 has a broader linear range and time-saving, so we chose M1 for further research. Moreover, the comparison of performances of different immunosensor which reported recently is shown in Table S3. The results indicated that the proposed strategy was a promising candidate for quantitative recognition of m6A-RNA.

As an analytical method, detection specificity is an important property. In order to investigate the specificity of the proposed method for m6A-RNA detection, some interferences were selected including single-stranded DNA (L1') which has the same sequences with L1 but without any modification, P2 and P3 with the same sequences to P1, P2 with a modification of 5-methylcytosine (5-mC) and P3 with no modification, dNTPs (dATP, dTTP, dCTP, dGTP) and a mixture solution (P2 + P3 + dNTPs). As shown in Fig. 5A, compared with the blank (PBS + 5 nM L1) and P1 + L1 (10 nM P1 + 5 nM L1), all of the interferences showed no clear effects on the test results at the concentration of 1 μM interferences (P2, P3, dNTPs or Mixture) + 5 nM L1. The results of 1 μM L1' revealed that the immunosensor has almost no nonspecific adsorption of nucleic acid, and the EIS responses are caused by the anti-m6A-Abs specific recognition of m6A. These results indicated that the proposed electrochemical immunosensor displayed a high specificity towards m6A.

3.4. Reproducibility and stability of the biosensor

Reproducibility is another key parameter for the biosensor. The reproducibility among the electrodes was tested. As shown in Fig. S4 ten immunosensors were prepared with the same process and tested at a concentrations of 10 nM P1 + 5 nM L1 and 200 nM P1 + 5 nM L1 with five repeat parallels. The relative standard deviations (RSD) are 0.59% and 0.73% (Table S4), respectively. The data suggested that this method has excellent reproducibility.

The stability of the fabricated immunosensor was also investigated. After the immunosensor was stored in a refrigerator at 4 °C for 7 days, 97.6% of its initial EIS response was retained. As expected, the new immunosensor has a satisfactory stability.

3.5. Biological samples detection

In order to prove the applicability of the proposed immunosensor, the content of m6A in total RNA, which extracted from HepG-2, L02, HBE and A549 were detected, respectively. For further proving the accuracy of the immunosensor in biological samples detection, the m6A content in the extracted total RNA samples were also tested by EpiQuik m6A RNA Methylation Quantification Kit. We have obtained a consistent result by comparing the two methods, shown in Fig. 5B. The results show a high consistency between the two methods.

4. Conclusions

In summary, a novel label-free electrochemical immunosensor was constructed for detection of m6A-RNA. An analogous modified DNA probe acts as a signal molecule, by competing with m6A-RNA for binding to Abs to broaden the linear range. The detection of m6A-RNA by this method is not affected by the lengths and base sequences of RNA. The fabricated immunosensor showed a wide linear range from 0.05 to 200 nM with a low detection limit of 0.016 nM. In addition, the immunosensor has successfully implemented the detection of total RNAs extracted from HepG-2, L02, HBE and A549. However, this method still has some deficiencies such as: the sensitivity is not high enough to detect some very low levels of RNA modifications, and it cannot detect RNA modifications other than m6A. In the future, we will work hard to improve the deficiencies of this method, and build a potential assay platform that can be used for RNA modifications.

Acknowledgments

This work was financially supported by National Natural Science Foundation of China (Nos. 81672112 and 81702101), the Key project of

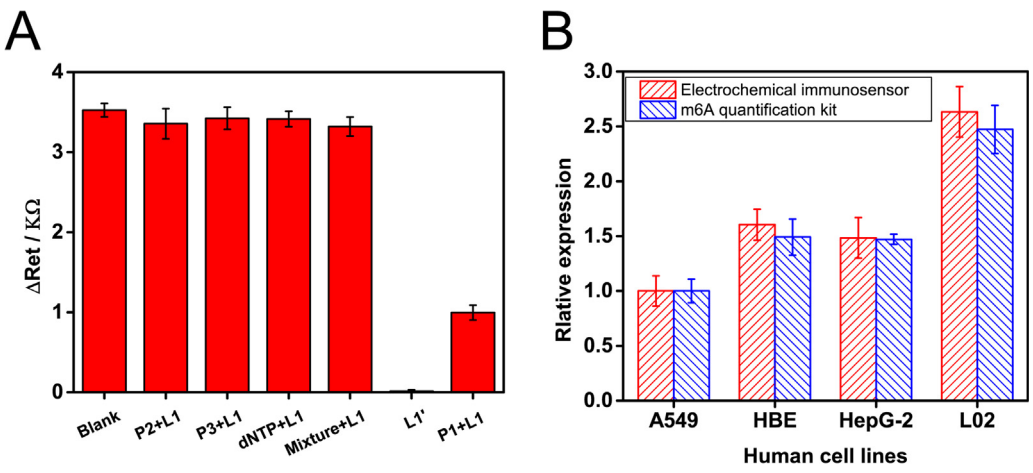

Fig. 5. (A) The electrochemical response of the immunosensor with different kinds of nucleotides: blank (PBS + 5 nM L1), P2 + L1 (1 μM P2 + 5 nM L1), P3 + L1 (1 μM P3 + 5 nM L1), dNTPs + L1 (1 μM dNTPs + 5 nM L1), Mixture + L1 (1 μM Mixture + 5 nM L1), L1' (1 μM L1'), P1 + L1 (10 nM P1 + 5 nM L1). (B) The relative expression of m6A in different human cell lines.

Education Department of Sichuan (No. 16ZA0181) and Key project of Health and Family Planning Commission of Sichuan Province (No. 16ZD036).

Appendix A. Supplementary material

Supplementary data associated with this article can be found in the online version at http://dx.doi.org/10.1016/j.bios.2018.05.018.

References

Bellodi, C., McMahon, M., Contreras, A., Juliano, D., Kopmar, N., Nakamura, T., Maltby, D., Burlingame, A., Savage, S.A., Shimamura, A., Ruggero, D., 2013. Cell Rep. 3 (5), 1493–1502.
Benvidi, A., Jahanbani, S., 2016. J. Electroanal. Chem. 768, 47–54.
Benvidi, A., Rajabzadeh, N., Mazloum-Ardakani, M., et al., 2014. Biosens. Bioelectron. 58 (58), 145.
Benvidi, A., Tezerjani, M.D., Jahanbani, S., et al., 2016. Talanta 147, 621–627.
Casalini, S., Dumitru, A.C., Leonardi, F., Bortolotti, C.A., Herruzo, E.T., Campana, A., de Oliveira, R.F., Cramer, T., Garcia, R., Biscarini, F., 2015. ACS Nano 9 (5), 5051–5062.
Chandola, U., Das, R., Panda, B., 2015. Brief. Funct. Genom. 14 (3), 169–179.
Chen, M., Wei, L., Law, C.T., Tsang, F.H., Shen, J., Cheng, C.L., Tsang, L.H., Ho, D.W., Chiu, D.K., Lee, J.M., Wong, C.C., Ng, I.O., Wong, C.M., 2017. Hepatology.
Dominissini, D., Moshitch-Moshkovitz, S., Schwartz, S., Salmon-Divon, M., Ungar, L., Osenberg, S., Cesarkas, K., Jacob-Hirsch, J., Amariglio, N., Kupiec, M., Sorek, R., Rechavi, G., 2012. Nature 485 (7397), 201–206.
Gao, F., Fan, T., Ou, S., Wu, J., Zhang, X., Luo, J., Li, N., Yao, Y., Mou, Y., Liao, X., Geng, D., 2018. Biosens. Bioelectron. 99, 201–208.
Geula, S., Moshitch-Moshkovitz, S., Dominissini, D., Mansour, A.A., Kol, N., Salmon-Divon, M., Hershkovitz, V., Peer, E., Mor, N., Manor, Y.S., Ben-Haim, M.S., Eyal, E., Yunger, S., Pinto, Y., Jaitin, D.A., Viukov, S., Rais, Y., Krupalnik, V., Chomsky, E., Zerbib, M., Maza, I., Rechavi, Y., Massarwa, R., Hanna, S., Amit, I., Levanon, E.Y., Amariglio, N., Stern-Ginossar, N., Novershtern, N., Rechavi, G., Hanna, J.H., 2015. Science (New York, N.Y.) 347 (6225), 1002–1006.
Gilbert, W.V., Bell, T.A., Schaening, C., 2016. Science (New York, N.Y.) 352 (6292), 1408–1412.
Helm, M., Motorin, Y., 2017. Nat. Rev. Genet. 18 (5), 275–291.
Ji, Y., Zhang, L., Zhu, L., Lei, J., Wu, J., Ju, H., 2017. Biosens. Bioelectron. 96, 201–205.
Jia, G., Fu, Y., Zhao, X., Dai, Q., Zheng, G., Yang, Y., Yi, C., Lindahl, T., Pan, T., Yang, Y.G., He, C., 2011. Nat. Chem. Biol. 7 (12), 885–887.
Jing, X., Cao, X., Wang, L., Lan, T., Li, Y., Xie, G., 2014. Biosens. Bioelectron. 58, 40–47.
Kan, L., Grozhik, A.V., Vedanayagam, J., Patil, D.P., Pang, N., Lim, K.S., Huang, Y.C., Joseph, B., Lin, C.J., Despic, V., Guo, J., Yan, D., Kondo, S., Deng, W.M., Dedon, P.C., Jaffrey, S.R., Lai, E.C., 2017. Nat. Commun. 8, 15737.
Klungland, A., Dahl, J.A., 2014. Curr. Opin. Genet. Dev. 26, 47–52.
Li, J., Chen, Z., Xiang, Y., Zhou, L., Wang, T., Zhang, Z., Sun, K., Yin, D., Li, Y., Xie, G., 2016a. Biosens. Bioelectron. 86, 75–82.
Li, X., Xiong, X., Yi, C., 2016b. Nat. Methods 14 (1), 23–31.
Linder, B., Grozhik, A.V., Olarerin-George, A.O., Meydan, C., Mason, C.E., Jaffrey, S.R., 2015. Nat. Methods 12 (8), 767–772.
Lv, M., Liu, Y., Geng, J., Kou, X., Xin, Z., Yang, D., 2018. Biosens. Bioelectron.
Ma, J.Z., Yang, F., Zhou, C.C., Liu, F., Yuan, J.H., Wang, F., Wang, T.T., Xu, Q.G., Zhou, W.P., Sun, S.H., 2017. Hepatology 65 (2), 529–543.
Meyer, K.D., Jaffrey, S.R., 2014. Nat. Rev. Mol. Cell Biol. 15 (5), 313–326.
Meyer, K.D., Saletore, Y., Zumbo, P., Elemento, O., Mason, C.E., Jaffrey, S.R., 2012. Cell 149 (7), 1635–1646.
Nainar, S., Marshall, P.R., Tyler, C.R., Spitale, R.C., Bredy, T.W., 2016. Nat. Neurosci. 19 (10), 1292–1298.
Narayan, P., Ludwiczak, R.L., Goodwin, E.C., Rottman, F.M., 1994. Nucleic Acids Res. 22 (3), 419–426.
Nelson, M.A., Reiter, W.S., Hage, D.S., 2003. Biomed. Chromatogr. 17 (2–3), 188–200.
Shen, H., Yang, J., Chen, Z., Chen, X., Wang, L., Hu, J., Ji, F., Xie, G., Feng, W., 2016. Biosens. Bioelectron. 81, 495–502.
Silva, N.F.D., Magalhaes, J., Freire, C., Delerue-Matos, C., 2018. Biosens. Bioelectron. 99, 667–682.
Slotkin, W., Nishikura, K., 2013. Genome Med. 5 (11), 105.
Tang, S., Shen, H., Hao, Y., Huang, Z., Tao, Y., Peng, Y., Guo, Y., Xie, G., Feng, W., 2018. Biosens. Bioelectron. 104, 72–78.
Tao, Y., Yin, D., Jin, M., Fang, J., Dai, T., Li, Y., Li, Y., Pu, Q., Xie, G., 2017. Biosens. Bioelectron. 96, 99–105.
Visvanathan, A., Patil, V., Arora, A., Hegde, A.S., Arivazhagan, A., Santosh, V., Somasundaram, K., 2018. Oncogene 37 (4), 522–533.
Vu, L.P., Pickering, B.F., Cheng, Y., Zaccara, S., Nguyen, D., Minuesa, G., Chou, T., Chow, A., Saletore, Y., MacKay, M., Schulman, J., Famulare, C., Patel, M., Klimek, V.M., Garrett-Bakelman, F.E., Melnick, A., Carroll, M., Mason, C.E., Jaffrey, S.R., Kharas, M.G., 2017. Nat. Med. 23 (11), 1369–1376.
Wang, L., Stegemann, J.P., 2010. Biomaterials 31 (7), 1612.
Wang, X., Lu, Z., Gomez, A., Hon, G.C., Yue, Y., Han, D., Fu, Y., Parisien, M., Dai, Q., Jia, G., Ren, B., Pan, T., He, C., 2014. Nature 505 (7481), 117–120.
Wang, X., Zhao, B.S., Roundtree, I.A., Lu, Z., Han, D., Ma, H., Weng, X., Chen, K., Shi, H., He, C., 2015. Cell 161 (6), 1388–1399.
Wang, X., Yang, C., Zhu, S., Yan, M., Ge, S., Yu, J., 2017. Biosens. Bioelectron. 87, 108–115.
Xiang, Y., Laurent, B., Hsu, C.H., Nachtergaele, S., Lu, Z., Sheng, W., Xu, C., Chen, H., Ouyang, J., Wang, S., Ling, D., Hsu, P.H., Zou, L., Jambhekar, A., He, C., Shi, Y., 2017. Nature 543 (7646), 573–576.
Yan, M., Wang, Y., Hu, Y., Feng, Y., Dai, C., Wu, J., Wu, D., Zhang, F., Zhai, Q., 2013. Anal. Chem. 85 (24), 12173–12181.
Yin, H., Zhou, Y., Yang, Z., Guo, Y., Wang, X., Ai, S., Zhang, X., 2015. Actuators B-Chem. 221, 1–6.
Yin, H., Wang, H., Jiang, W., Zhou, Y., Ai, S., 2017. Biosens. Bioelectron. 90, 494–500.
Zeng, G., Zhang, C., Huang, D., Lai, C., Tang, L., Zhou, Y., Xu, P., Wang, H., Qin, L., Cheng, M., 2017. Biosens. Bioelectron. 90, 542–548.
Zhang, C., Chen, Y., Sun, B., Wang, L., Yang, Y., Ma, D., Lv, J., Heng, J., Ding, Y., Xue, Y., Lu, X., Xiao, W., Yang, Y.G., Liu, F., 2017. Nature 549 (7671), 273–276.
Zhang, X., Cozen, A.E., Liu, Y., Chen, Q., Lowe, T.M., 2016. Trends Mol. Med. 22 (12), 1025–1034.
Zhao, M., Zhang, S., Chen, Z., Zhao, C., Wang, L., Liu, S., 2018. Biosens. Bioelectron. 105, 42–48.
Zhao, X., Yang, Y., Sun, B.F., Shi, Y., Yang, X., Xiao, W., Hao, Y.J., Ping, X.L., Chen, Y.S., Wang, W.J., Jin, K.X., Wang, X., Huang, C.M., Fu, Y., Ge, X.M., Song, S.H., Jeong, H.S., Yanagisawa, H., Niu, Y., Jia, G.F., Wu, W., Tong, W.M., Okamoto, A., He, C., Rendtlew Danielsen, J.M., Wang, X.J., Yang, Y.G., 2014. Cell Res. 24 (12), 1403–1419.